Channel Modeling and Characterization at 17 GHz for Indoor Broadband WLAN

Manuel Lobeira Rubio, Ana García-Armada, *Member, IEEE*, Rafael P. Torres, *Member, IEEE*, and José Luis García, *Member, IEEE*

***Abstract*—This paper provides the results of a complete study about the indoor radio propagation channel at 17 GHz. Wideband parameters, as coherence bandwidth or rms delay spread, and coverage are analyzed for the design of an OFDM-based broadband WLAN. Discussion about some adequate system parameters is also included. The report presents the characterization results as well as a recently developed indoor channel model; both of them have been checked and compared to bibliography results in order to verify their reliability.**

***Index Terms*—17-GHz indoor channel, channel characterization, channel modeling, fading channels, indoor communications, OFDM, wireless LAN.**

I. Introduction

IN THE framework of the European Information Society Technologies (IST) program, the purpose of the WIND-FLEX Project (IST-1999-10 025) is the development of a very flexible wireless indoor modem with a bit rate between 64 kb/s and 100 Mb/s for small office–home office (SOHO) environments with low mobility. Orthogonal frequency-division multiplexing (OFDM) has been adopted for the air interface as a mean of combating multipath in such environments. The operating carrier frequency is 17 GHz and the selected bandwidth channel is 50 MHz. This paper presents the results obtained from the complete study carried out in the context of the WIND-FLEX project to deduce the range, the number, and separation of the OFDM subcarriers and cyclic prefix duration among other parameters. The initial tested ranges were 10 m for nonline-of-sight (NLOS) paths and 20 m for line of sight (LOS) scenarios.

The work has been divided into two parts: in the first part, the method used to obtain the channel parameters is described and, in the second part, the deductions leading to the selection of a channel model for indoor environments at 17 GHz is outlined. The parameters have been extracted using the CINDOOR simulator [1] developed by the University of Cantabria. This simulator is a site-specific propagation model based on three-dimensional (3-D) ray-tracing techniques, which has been specifically developed for simulating radio coverage and channel performance in enclosed spaces such as buildings, and for urban microcell and picocell calculations. The simulator requires the input of the geometric structure and the electromagnetic properties of the propagation environment, and is based on a full 3-D implementation of geometric optics and the uniform theory of diffraction (GO/UTD). The simulator results and the accuracy achievable have been verified in previous works at different frequencies obtaining very accurate results for narrowband as well as for wideband parameters [2], [3]. For the band of 1.8 and 2.5 GHz, the authors have carried out an extensive measurement campaign [4]; for other bands, the results have been tested by comparison with data in the literature. In fact, the reliability of the predictions at 17 GHz has been tested by means of comparisons between some channel parameters that are reported in the available literature and those obtained by the method proposed here.

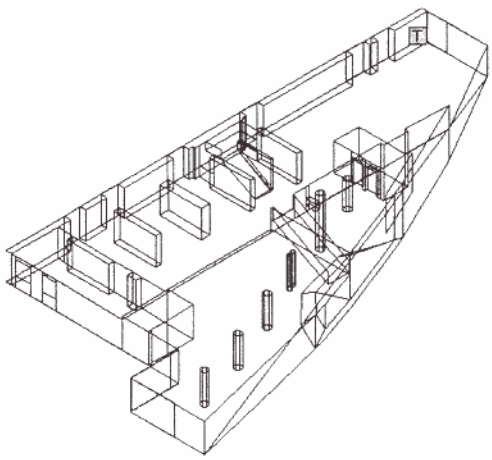

Fig. 1. ETSIIT hall (49 m × 26 m).

The proposed channel model will consist of a dicretized multibin channel impulse response. The variability of the bin amplitudes is modeled by the statistical distributions that best fit the data obtained by simulating impulse responses in a dense grid of points along the areas of interest.

II. Channel Characterization

Three different scenarios have been studied representing typical ones: a hall as a wide indoor area, offices separated by soft materials and located on two adjacent floors and a seven-story office building. These scenarios are presented in Figs. 1–3.

This work was supported in part by the European Commission and in part by the Spanish National Plan projects WIND-FLEX (IST-1999-10025) and CICYT-2FD97-1066-C02-02.

M. Lobeira Rubio is with ACORDE S.A., Centro de Desarrollo Tecnológico, Universidad de Cantabria, 39005 Santander, Spain (e-mail: mlobeira@acordecom.com).

A. García-Armada is with the Dpt. Tecnologías de las Comunicaciones, University Carlos III of Madrid, Leganes 28911, Spain (e-mail: agarcia@tsc.uc3m.es).

R. P. Torres and J. L. García are with the Dpt. Ingeniería de Comunicaciones, ETSII Telecomunicación, University of Cantabria, 39005 Santander, Spain (e-mail: rtorres@dicom.unican.es; jlgarcia@dicom.unican.es).

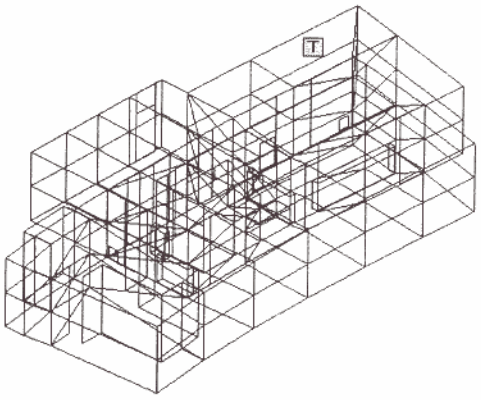

Fig. 2. DICOM, floors −2 and −3 (34 m × 20 m).

Two types of analysis have been carried out: coverage and power delay profiles. The following propagation mechanisms or rays coupling the transmitter and the receiver have been considered during the simulation process: direct, reflected, diffracted, reflected–diffracted, diffracted–reflected, double reflected, and triple reflected rays. The authors' experience is that these rays are sufficient to obtain accurate results in normal offices and in residential environments; in general, in buildings without a high density of metallic machinery [2], [4]. Due to the communication characteristics (mobility lower than 1 m/s), the Doppler effect will be obviated.

A. Wideband Parameters

The first part of the study analyzes wideband parameters: coherence bandwidth (Bc), maximum delay ($T\,\max$), and rms delay spread ($\tau_{\rm rms}$).

1) Coherence Bandwidth: This parameter is directly obtained from the simulation tool; in the frequency domain the channel can be characterized using the autocorrelation function, which is the Fourier transform of the mean power delay profile [1]. The mean and standard deviation of the coherence bandwidth have been obtained for the three scenarios of Figs. 1–3, with values between about 24 MHz for wide areas to about 14 MHz for the offices with soft separation, these values being for a 50% correlation. These values are shown in Table I and the cumulative distribution function (CDF) is shown in Fig. 4.

To understand the implications of these results we have to consider the maximum bit rate, 100 Mb/s, specified in WINDFLEX, using the most efficient modulation (64QAM), which leads to a 16.7-MHz signal bandwidth [5]

$$B(\text{Hz}) = \frac{R(\text{b/s})}{\eta(\text{b/s/Hz})} = \frac{100\ \text{Mb/s}}{6\ \text{b/s/Hz}} = 16.67\ \text{MHz}. \qquad (1)$$

It can be observed in Fig. 4 that the coherence bandwidth of the channel is lower than that required at 16.7 MHz for 52% of the time. This situation deteriorates if the overhead from higher OSI layers and coding are included in the calculations. For this reason, a single carrier scheme is not adequate unless a complex equalizer is used with it, so that multicarrier system such as OFDM must be employed.

Once the CDF curve is obtained, the value that must be used for the system design is the worst one, which is the minimum, which in our case is 2.41 MHz. The reliability of these results can be further verified by comparison to [6], which includes the results of measurements in indoor scenarios similar to those of this paper and working at the same frequency. The value given in [6] for the coherence bandwidth was 2.22 MHz, very close to our result of 2.41 MHz.

A further requirement related to the correct and efficient channel estimation process by the receiver is the selection of a number of subcarriers satisfying the condition of being separated between approximately $Bc/5$ and $Bc/10$, which leads to a scheme of 128 subcarriers. Moreover, since the signal bandwidth is fixed at 50 MHz, there will be a symbol duration of 2.56 ms. The main advantage of using OFDM in frequency-selective channels is that the number of subcarriers can be selected so that the channel is flat in each subchannel leading to a very simple one-tap equalization. This is possible if we select a number of subcarriers satisfying the condition of being separated less than Bc. Moreover, in order to be able to estimate the channel correctly for this equalization, it is desirable that there exists some correlation in channel values among adjacent subchannels. For instance, some OFDM schemes use several subcarriers as pilots, so as to estimate the channel. In these systems, in order to achieve a good channel estimation without a serious reduction in transmission rate, a separation of $Bc/5$ to $Bc/10$ constitutes a good tradeoff [7].

2) RMS Delay Spread (RDS): The second of the wideband parameters, the rms delay spread, has a similar behavior to coherence bandwidth: high standard deviation around the mean value; and for that reason we have obviated the representation of the mean values, presenting directly its CDF (see Fig. 5 and Table II).

The reliability of these results, mean value of 21.78 ns and standard deviation of 12.94 ns, can be verified in [8], [9], or [10]. The first reference describes the measurements carried out by Delft University and provides a mean value of 20.74 ns, and values ranging from 5 to 70 ns. The second presents a mean value of 20 ns, and values ranging from 10–50 ns, while the third reference gives a mean value of 19 ns.

3) Maximum Delay: Another point of interest is the study of the maximum delay in the multipath propagation which influences the minimum cyclic prefix of the OFDM symbol. The total communication delay, including the propagation delay, has been considered, that is

$$T_{\text{MAX-Comm}} = T_{\text{MAX-Channel}} + \frac{d_{TX-RX}}{c} \qquad (2)$$

where $T_{\text{MAX-Comm}}$ is the complete duration of the communication, that is, the duration of the channel response considered on a threshold basis, $T_{\text{MAX-Channel}}$, added to the propagation delay, being d_{TX-RX} the distance between the transmitter and the receiver while c is the speed of light.

Two different processes have been carried out in order to calculate the duration of the channel response. The first one has discarded the power delay profile (PDF) components whose amplitudes are 30 dB (or more) lower than the maximum. The second process is similar, but it counts only components up to 20 dB below the maximum. Figs. 6 and 7 show the results obtained by

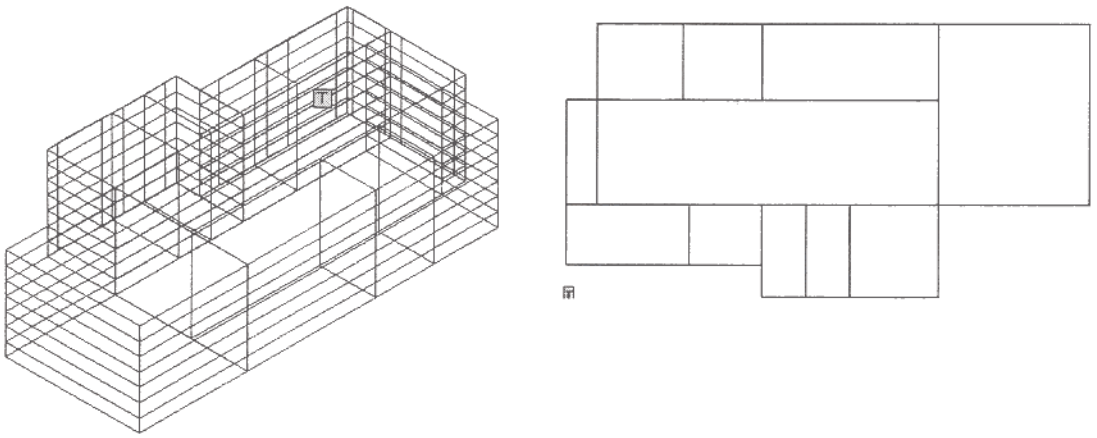

Fig. 3. Office building (72 m × 38 m), 2-D and 3-D representations.

TABLE I
Bc AT 17 GHz

Place	Coherence Bandwidth (MHz)	
	Mean	Standard deviation
Hall	24.85	12.35
Floors	14.44	9.85
Building	22.86	10.24
Total	20.72	11.56

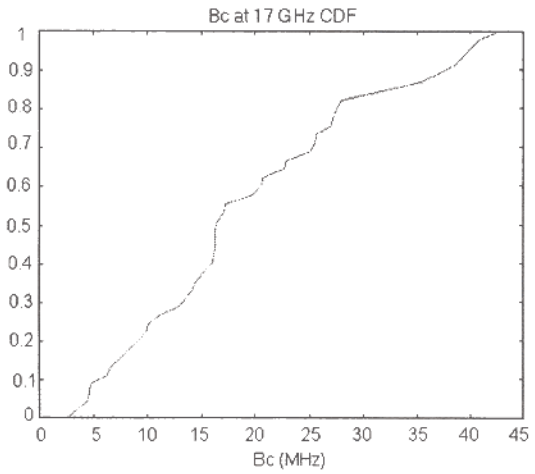

Fig. 4. Bc CDF at 17 GHz.

the two processes for 17 GHz. Tables III and IV show the value of maximum delay for several CDF values.

It can be seen that 200 ns is the maximum value obtained for the most restrictive criterion; due to the small difference introduced in the efficiency over the 2.56 μs of OFDM symbol by the two different criteria, we propose this value, 200 ns, as the cyclic prefix duration.

The maximum delay is not a standard parameter itself, although it has been used here in order to define the OFDM guard times, so it is not appropriate to verify its reliability now. Nevertheless, we will address this subject in the section on the channel model results.

4) Relationship Between Bc and RDS, Alpha Parameter: The relationship between the coherence bandwidth (Bc)

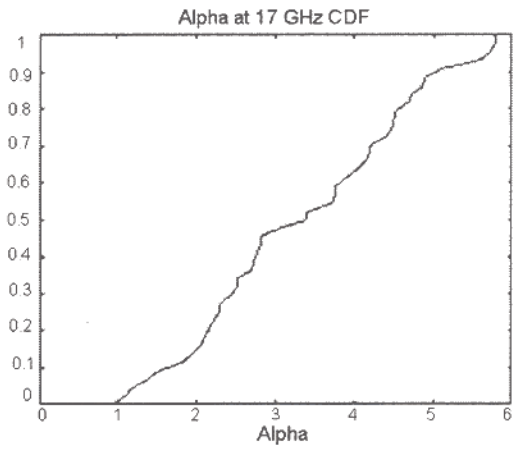

Fig. 5. RMS delay spread CDF.

TABLE II
RMS DELAY SPREAD CDF

CDF Value	RDS Value
0.2	12.1 ns
0.4	14.3 ns
0.6	17.5 ns
0.8	34.3 ns
1	58.3 ns

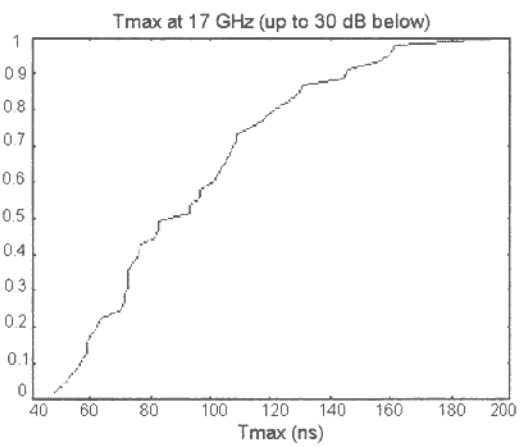

Fig. 6. Maximum Delay CDF, 30 dB criterion.

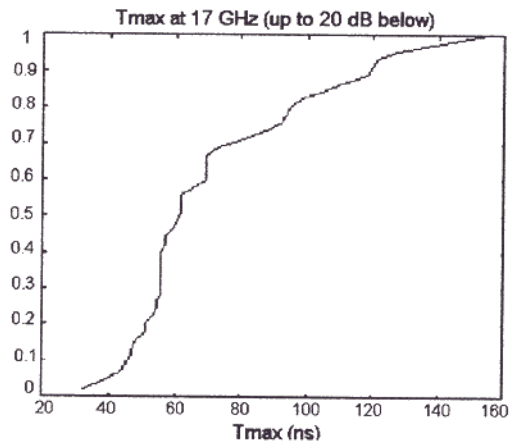

Fig. 7. Maximum Delay CDF, 20 dB criterion.

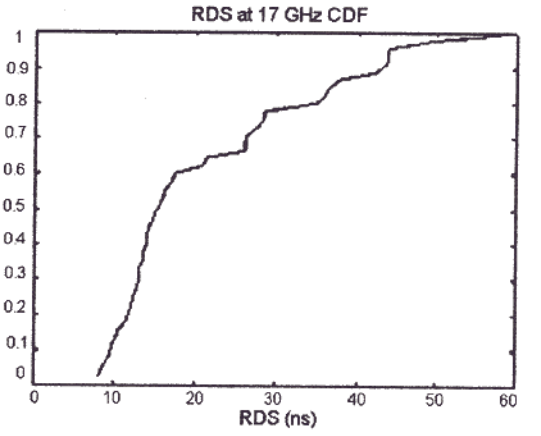

Fig. 8. Alpha CDF.

TABLE III
MAXIMUM DELAY CDF, 30 dB CRITERION

CDF Value	Tmax Value
0.2	62 ns
0.4	76 ns
0.6	101 ns
0.8	122 ns
1	197 ns

TABLE IV
MAXIMUM DELAY CDF, 20 dB CRITERION

CDF Value	Tmax Value
0.2	51 ns
0.4	56 ns
0.6	69 ns
0.8	94 ns
1	156 ns

TABLE V
ALPHA CDF

CDF Value	Alpha Value
0.2	2.17
0.4	2.67
0.6	3.75
0.8	4.44
1	5.78

at 50% and the rms delay spread has also been studied, using the nondimensional parameter α, with the implicit definition $Bc = 1/\alpha\tau_{\rm rms}$, whose CDF is shown in Fig. 8 and Table V.

This CDF, with 3.35 as mean value, presents a more optimistic relationship than the one shown in [11], $Bc \approx 1/5\tau_{\rm rms}$, which allows, for a constant signal bandwidth, a wider range of $\tau_{\rm rms}$values without suffering selective fading. This is not a common parameter, so it has been impossible to find in the bibliography any other study at 17 GHz to verify the reliability of these results.

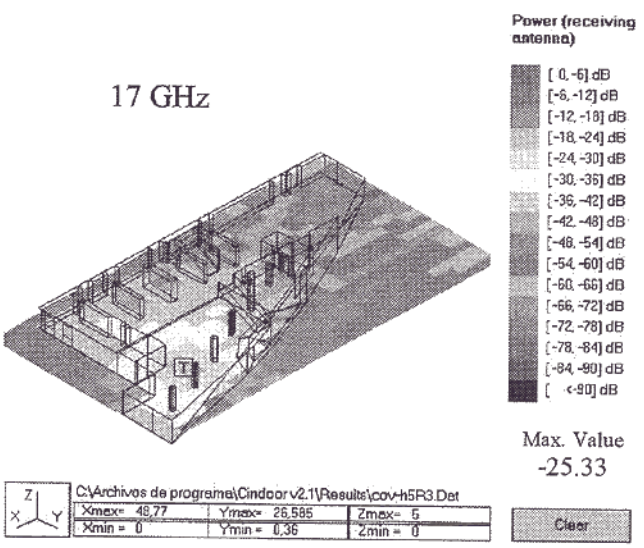

Fig. 9. Coverage map for the hall, with EIRP= 10 dBm.

B. Coverage

1) Path Loss Exponent: The path loss model assumes the well-known exponential variation of the received power with the distance [12]. The values of the exponent have been obtained using a reference distance, d_0, of 0.1 m, while the location of the antennas is approximately 1.1 m high, assuming a desk use.

The path loss exponent deduced in this work is close to two (2, 2.1) in wide areas and obstructed line of sight (in which diffraction allows the arrival of components which have not passed through any obstacle) scenarios. For NLOS cases (offices of about 40 m^2 separated of other similar ones by brick walls of 10 to 15 cm) the mean value of the path loss exponent is approximately 2.6. Simulations carried out in this report for the LOS case inside rooms up to 120 m^2 have obtained exponent values lower than the free space situation (2.0), which implies an indoor gain effect, as shown in Fig. 9. Fig. 10 shows a picture of the coverage area in one of the wide area scenarios, while Table VI presents the mean values of the path loss exponent for different type of paths.

Several reports have obtained values closed to those of this report. Measurements presented by Delft University provided a value for "n," in LOS paths, of 1.7. Other studies have obtained values of 1.6 [13], 1.67 [14] and between 1.5 and 1.8 [15], [16]

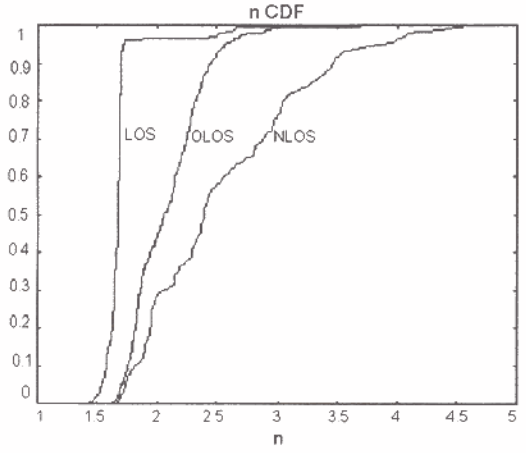

Fig. 10. CDF of path loss exponent "n."

TABLE VI
MEAN VALUES OF "n"

Type of Path	LOS	OLOS	NLOS
'n' Mean value	1.68	2.14	2.61

TABLE VII
FADING STATISTICS OVER DISTANCE, LOS CASE

Radius (m)	K factor
4	17
5	10
6	9
7	8
8	6
9	5
10	1

for similar situation. For NLOS case, the Delft University results lead to a global mean of 2.93. Their report obtained values lower than 2.0 for NLOS paths, as we did. References [15] and [16] presented values ranging from 2.4 to 2.8, an interval which includes the mean value obtained in this work.

2) Narrowband Fading Statistics: As well as the mean values of received power, it is also of interest to verify the variations around them in order to assure a certain quality of service (QoS), providing the required level of transmitted power. Thus, several situations have been analyzed in order to characterize the narrowband fading statistics in the indoor environment at 17 GHz. The first one has evaluated the LOS case over a circular path with increasing radius. The results are shown in Table VII, while the scenario appears in Fig. 11. Table VII shows the value of K, the Ricean factor, that best fits the fading statistics.

It may come as a surprise that a Rayleigh distribution is obtained for fading in the LOS case, but this fact can be easily explained. In a complex scenario like a SOHO environment, where a rich scattering exists, the multipath signal level is practically constant. However, at short distances from the transmitter, the direct ray signal power quickly decreases as the distance from the transmitter increases. Thus, the ratio between the direct ray and the rest of the multipath components decreases as the distance (inside a room) increases, leading to a Rayleigh distribution. The reliability of these results can be verified through [17], a report that presents measurements of the indoor radio channel

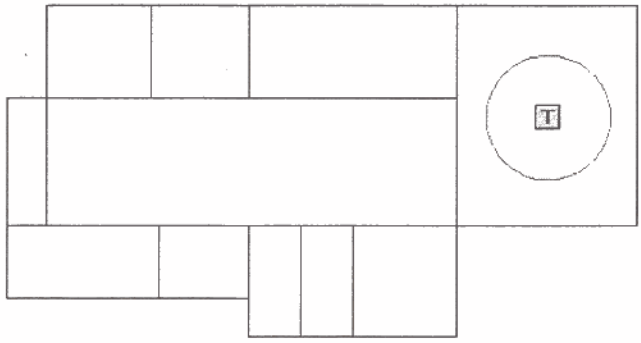

Fig. 11. Scenario for evaluating the LOS case.

TABLE VIII
FADING STATISTICS OVER DISTANCE; NLOS CASE

Radius (m)	K factor
4	17
6	12
8	7
10	1

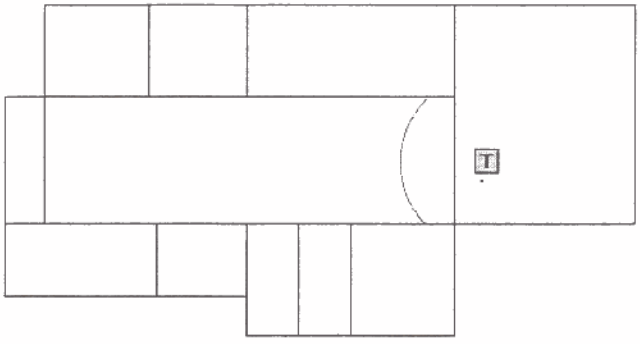

Fig. 12. Scenario for evaluating the NLOS case.

at 10 GHz. The measurements show that LOS cases with small distance followed a Rice distribution, but that, as the distance increases, the distribution changes to a Rayleigh one.

The same behavior can be found when analyzing the NLOS case, as shown below, in Table VIII and Fig. 12.

The similarities between the LOS and NLOS results are due to the distances and scenarios used in the process, because the only distinction is the presence of a wall in the path (for the NLOS path), which provokes a difference in the mean level of the received power but not different variations around it. With increasing distance, a variable number of walls for the different NLOS paths will appear, allowing distinction between the results of these two path cases.

These results will have a strong influence on the design of the system, due to the huge increment required in the transmitted power (Eb/No, [18]) in order to maintain, over a Rayleigh channel, the same error probability as a Gaussian channel.

III. CHANNEL MODEL

A. Modeling Process

The channel model has been obtained from CINDOOR simulations over a new scenario (Fig. 13) that best fits the future applications of the WIND-FLEX project. Different materials

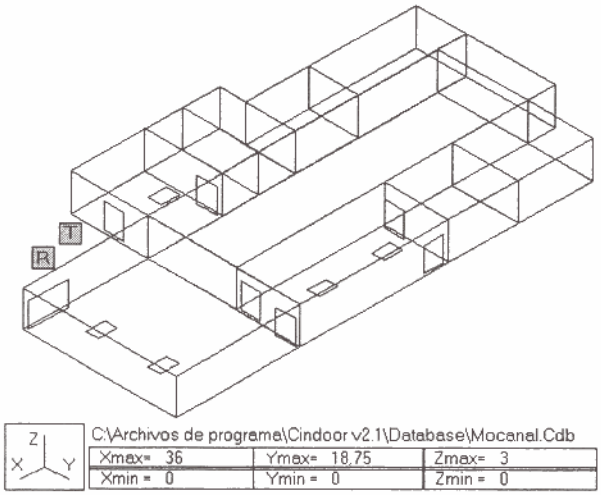

Fig. 13. WIND-FLEX scenario (36 m × 19 m).

as brick, metallic glass, soft internal walls, or wooden surfaces have been considered. The power delay profile (PDP) has been calculated by using a 3 ns resolution, which corresponds with a commonly achievable experimental resolution. This PDP will be discretized and adjusted into a bins model.

Narrowband situations can be modeled with only one bin, whose amplitude variation follows a Rayleigh or Rice probability density function. For wideband cases, a multipath (multibin) model is required. The difference between these situations lies in the relationship between the signal bandwidth and the channel one. A narrowband signal has a lower bandwidth than the channel coherence bandwidth.

In order to simulate the performance of different systems with different signal bandwidths, a bin size must be chosen which is equal to half the transmitted pulse duration in order to represent a PDP continuous function with the resolution defined by the pulse duration. Since the PDP duration is considered as a constant, the shorter the transmitted pulse, the higher the number of bins, leading to an increasing computational charge for the following simulation process. The bins will be placed in the temporal axis as follows:

$$T_i = T_{\text{PROP}} + (i - (1/2)) * T_{\text{BIN}} \qquad i = 1, 2, \ldots, N_{\text{BINS}} \quad (3)$$

where T_i represents the instant of time where the center of the ith bin of the channel model is placed, T_{PROP}, the propagation delay, calculated as the distance between the transmitter and the receiver divided by the speed of light, and T_{BIN} the bin duration.

Thus, the total duration for the modeled PDP is $N_{\text{BINS}} * T_{\text{BIN}}$. The amplitude of this PDP is adjusted to represent the channel response once free space losses have been subtracted. Since free space losses and propagation time are functions of the distance and the frequency, known for every situation, the model can be easily applied. Finally, with the time in seconds, the mean power received is

$$P_{RX}|_{\text{dB}} = P_{TX}|_{\text{dB}} + G_{TX}|_{\text{dB}} + G_{RX}|_{\text{dB}} - Lfs|_{\text{dB}} + 10 \cdot \log\left(\int_0^{\infty} \text{PDP}(t).dt\right) \quad (4)$$

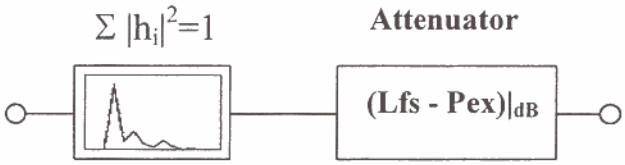

Fig. 14. Blocks diagram for simulation.

where P_{RX} represents the mean received power (extracted with the receiving antenna), P_{TX}, the mean power at the transmitting antenna input, G_{TX}, the transmitting antenna gain while G_{RX} is the receiving antenna gain, L_{fs}, free space propagation losses, given by $L_{fs}|_{\text{dB}} = 32.45 \text{ dB} + 20 \cdot \log_{10}(d_{\text{Km}} \cdot f_{\text{MHz}})$ and $\text{PDP}(t)$, the modeled power delay profile.

Once the PDP is modeled, to obtain the discrete channel impulse response, h_i, we only have to add a random phase to the square root of each bin amplitude, as follows:

$$h_i = \sqrt{p_i} \cdot e^{j\phi_i} \qquad \phi_i \;\; r.v. \;\; unif\,[0, 2\pi] \quad (5)$$

where h_i, is the ith bin of the modeled channel impulse response and p_i, the module of the ith bin of the modeled power delay profile.

It can be assumed that phases of different components of the same channel impulse response are uncorrelated at the frequency of interest (17 GHz), because their relative range is higher than a wavelength, even for high resolution models [19].

To implement this model on a simulator like ADS, SPW, or Matlab, the block diagram shown in Fig. 14 will be used, where P_{ex}, represents the excess power, that is, the power received in excess over the free space situation. The first block represents the normalized channel impulse response, in order not to lose accuracy during the convolution process. The second block is an attenuator for reducing the amplitude of the received signal with the proper propagation losses.

B. Wind-Flex Model

It is easy to verify that the model presented represents a static channel, that is, each realization will lead to a channel response that will not vary with time. The decision was made considering the ratio between the coherence time and the OFDM symbol duration. The maximum user speed is 1 m/s, which makes 2 m/s in the worst situation (both transmitter and receiver moving in the same direction but opposite ways). At 17 GHz, the maximum Doppler shift will be 114 Hz, which will lead to a coherence time of 3.71 ms, using the following expression [20], where f_m represents the maximum frequency of the Doppler spectrum:

$$T_C = \sqrt{\frac{9}{16 \cdot \pi \cdot f_m^2}} = \frac{0.423}{f_m}. \quad (6)$$

However, further studies [21] have presented a worst case value of 1 ms, which will be the one employed. With this coherence time, a great number of OFDM symbols can be transmitted without significant changes in the channel impulse response

$$N_{\text{SYMBOLS}} = \frac{T_C}{T_S + T_G} = \frac{1 \cdot 10^{-3}}{2.76 \cdot 10^{-6}} \cong 362 \quad (7)$$

TABLE IX
WIND-FLEX CHANNEL MODEL PDFS, LOS CASE

WIND-FLEX LOS Channel Model pdf's					
Bin 1	Frechet (σ =2.66e8,λ=7)	**Bin 4**	Exp. (σ=1.45e7)	**Bin 7**	Exp. (σ=0.41e7)
Bin 2	Exp. (σ=5.44e7)	**Bin 5**	Exp. (σ=1.03e7)	**Bin 8**	Exp. (σ=0.27e7)
Bin 3	Exp. (σ=2.51e7)	**Bin 6**	Exp. (σ=0.79e7)	**Bin 9**	Exp. (σ=0.71e7)

TABLE X
WIND-FLEX CHANNEL MODEL PDFS, NLOS CASE

WIND-FLEX NLOS Channel Model pdf's					
Bin 1	0.5*[Exp(σ=4.378e6) + Weibull (σ= 4.207e7, λ=5)]	**Bin 7**	Exp. (σ=1.88e5)	**Bin 13**	Exp. (σ=9.21e4)
Bin 2	Exp. (σ=3.04e6)	**Bin 8**	Exp. (σ=2.51e5)	**Bin 14**	Exp. (σ=1.27e5)
Bin 3	Exp. (σ=2.47e6)	**Bin 9**	Exp. (σ=5.69e5)	**Bin 15**	Exp. (σ=2.76e4)
Bin 4	Exp. (σ=2.14e6)	**Bin 10**	Exp. (σ=1.53e5)	**Bin 16**	Exp. (σ=6.71e4)
Bin 5	Exp. (σ=1.1e6)	**Bin 11**	Exp. (σ=3.29e5)	**Bin 17**	Exp. (σ=6.42e4)
Bin 6	Exp. (σ=3.71e5)	**Bin 12**	Exp. (σ=2.67e5)		

where T_S represents the duration of the information section in the OFDM, while T_G, is the guard time, the cyclic prefix of the OFDM symbol.

The small temporal variations in the channel impulse response could be introduced later in the simulation process. One of the possibilities is the generation of a new channel impulse response periodically each coherence time or with a shorter period. Moreover, it should be advisable to filter in order to smooth the transition between two consecutive realizations. In this way, we could model a quasi-static channel, which is the situation produced by people's movements [22].

In our project, although each subchannel has a narrowband behavior, the characterization of the whole group of subcarriers requires a wideband model. As the total bandwidth assigned to the communication is 50 MHz, a selection of 10 ns for the bin size must be made. Using 99% of the total power criterion for the maximum duration of the PDP, the former bin size selection leads to a total of nine taps for the LOS case and seventeen for the NLOS case.

The statistical variability of the bin amplitudes has been modeled following different probability density functions. Taking into account the fact that the area of service of future applications (SOHO) has small ranges, the variability have been analyzed considering a medium-scale, that is, the environment is divided in the LOS area and the NLOS one. In the LOS case, a Frechet PDF [23] is chosen for the first bin and exponential PDFs for the rest. These PDFs were considered the most suitable after a fitting process. The NLOS case needs a combination of exponential and Weibull PDFs for the first bin and exponential PDFs for the others. Tables IX and X show the probability density functions employed for LOS and NLOS channel models.

For both tables, the units of σ parameters are Hz (s^{-1}), while λ has no units. These units have no physical correlation but make the last term of (4) nondimensional, as it represents a factor scale between the free space behavior and the real one.

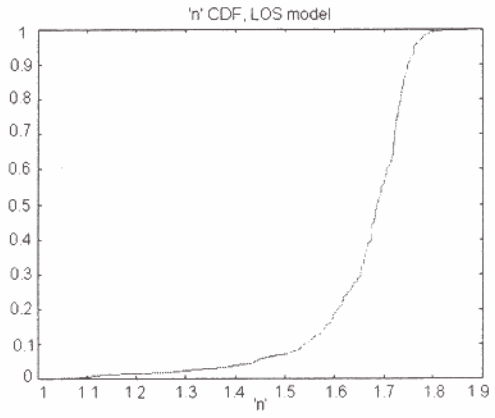

Fig. 15. Path loss exponent obtained with the LOS channel model.

The mean value of the probability density functions is so high due to the ulterior integral over the time (in seconds) required, and the PDP duration (tens of nanoseconds). As expected, the mean value of the first bin is the highest, since it includes the direct ray (LOS case).

C. Model Reliability

Once the channel model creation process is completed, that is, a statistical multibin model of the channel has been extracted from a collection of simulations, the reliability of the obtained statistical model should be verified. The channel was programmed using Matlab, and the following parameters (the most important ones for the ulterior design activities) have been chosen to verify the accuracy of the model: maximum delay, coherence bandwidth, path loss exponent, and fading statistics.

- *Maximum Delay:* depends on the number of bins and the distance between transmitter and receiver. The worst case appears when considering NLOS case and 10 m range, with a 203 ns result. This value is very close to the 200 ns one obtained in the characterization process. There is an external reference [24], which provides a maximum duration of 100 ns for the LOS channel response ($T_{\mathrm{MAX-Channel}}$) at 19 GHz, which is very close to our channel response: 90 ns, at 17 GHz.
- *Coherence Bandwidth:* the minimum value (NLOS case), the critical one, is 2.34 MHz, almost the same value as that obtained during the characterization, 2.41 MHz.
- *Path Loss Exponent:* the results for the LOS case appear in Fig. 15, with a mean value of 1.67, while the NLOS case resulted in 2.55. The accuracy achieved is very high when comparing these values to the characterization ones, 1.68 and 2.61.
- *Narrowband Fading Statistics:* the evaluation after the channel model simulations led to Ricean Statistical distributions for both cases, $K = 9$ in LOS case, and $K = 8$ for NLOS situations (Fig. 16). The problem with these results comes from the model creation process. The model has not developed a different set of probability density functions for each distance between transmitter and receiver, but rather for the mean behavior between short range and long range ones. For this reason, the fading statistics with a K factor equal to mean between

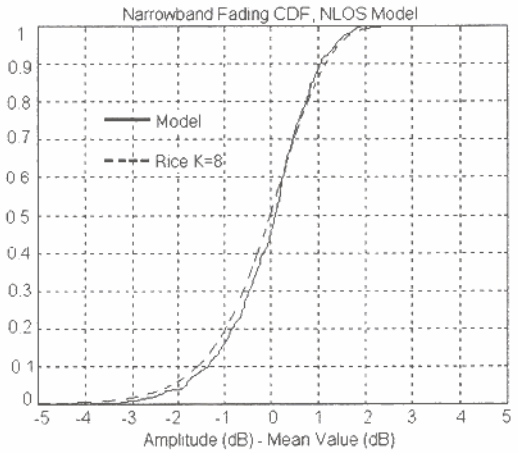

Fig. 16. Fading statistics obtained with the NLOS channel model.

the shortest distance, 1 m, ($K = 17$) and the maximum range ones ($K = 1$) is obtained. One possibility for improvement would be the introduction of a random variable, a function of the distance, to compensate the fading statistics.

IV. Conclusion

A complete study of the indoor radio channel at 17 GHz has been made, and the information obtained has been used to develop a statistical indoor radio channel model at that frequency. The reliability of all the parameters and results have been verified through the comparison with data found in the bibliography, reported from measurement campaigns. From the results presented, we can conclude the following.

- Maximum delay is no higher than 200 ns for a 10 m. maximum NLOS range.
- The path loss exponent, "n," mean value in LOS cases is lower than 2.0 (1.68), while a 2.6 mean value has been obtained for NLOS paths.
- Narrowband fading statistics are Rice at short distances and Rayleigh at large ones, even in LOS cases.

Appendix
Statistical Distributions (Extracted from [23])

FRECHET

A continuous random variable X has a Frechet distribution if its PDF has the form

$$f(x;\,\sigma;\,\lambda) = \frac{\lambda}{\sigma}\left(\frac{\sigma}{x}\right)^{\lambda+1}\exp\left\{-\left(\frac{\sigma}{x}\right)^{\lambda}\right\};$$
$$x \geq 0; \quad \sigma,\,\lambda > 0.$$

A Frechet variable X has the CDF

$$F(x;\,\sigma;\,\lambda) = \exp\left\{-\left(\frac{\sigma}{x}\right)^{\lambda}\right\}.$$

This model has a scale structure, with σ a scale parameter and λ a shape parameter.

WEIBULL

A continuous random variable X has a Weibull distribution if its PDF has the form

$$f(x;\,\sigma;\,\lambda) = \frac{\lambda}{\sigma}\left(\frac{x}{\sigma}\right)^{\lambda-1}\exp\left\{-\left(\frac{x}{\sigma}\right)^{\lambda}\right\}$$
$$x \geq 0; \quad \sigma,\,\lambda > 0.$$

While the CDF is

$$F(x;\,\sigma;\,\lambda) = 1 - \exp\left\{-\left(\frac{x}{\sigma}\right)^{\lambda}\right\}.$$

This model has a scale structure, that is, σ is a scale parameter, while λ is a shape parameter.

EXPONENTIAL

A continuous random variable X has a exponential distribution if its PDF has the form

$$f(x;\,\mu) = \frac{1}{\sigma}\cdot\exp\left\{-\left(\frac{x-\mu}{\sigma}\right)\right\}$$
$$x \geq 0; \quad \mu,\,\sigma > 0.$$

This PDF has location-scale structure, with a location parameter, μ, and a scale one, σ.

The CDF of the exponential variable X is

$$F(x;\,\mu) = 1 - \exp\left\{-\left(\frac{x-\mu}{\sigma}\right)\right\}.$$

References

[1] R. P. Torres, L. Valle, M. Domingo, S. Loredo, and M. C. Díez, "CINDOOR: An engineering tool for planning and design of wireless systems in enclosed spaces," *IEEE Antennas Propagat. Mag.*, vol. 41, pp. 11–22, Apr. 1999.

[2] S. Loredo, R. P. Torres, M. Domingo, L. Valle, and J. R. Pérez, "Measurements and predictions of the local mean power and small-scale fading statistics in indoor wireless environments," *Microwave Opt. Technol. Lett.*, vol. 24, pp. 329–331, Mar. 2000.

[3] R. P. Torres, S. Loredo, L. Valle, and M. Domingo, "An accurate and efficient method based on ray-tracing for the prediction of local flat-fading statistics in picocell radio channels," *IEEE J. Select. Areas Commun.*, vol. 18, pp. 170–178, Feb. 2001.

[4] S. Loredo, L. Valle, and R. P. Torres, "Accuracy analysis of GO/UTD radio channel modeling in indoor scenarios at 1.8 and 2.5 GHz," *IEEE Antennas Propagat. Mag.*, vol. 43, Oct. 2001.

[5] B. Sklar, *Digital Communications*, 2nd ed. Englewood Cliffs, NJ: Prentice-Hall, 2001, sec. 2.8.5, p. 92.

[6] A. Bohdanowicz, "Wide band indoor and outdoor radio channel measurements at 17 GHz," Ubicom, Tech. Rep./2000/2, Feb. 2000.

[7] L. Hanzo, W. Webb, and T. Keller, *Single- and Multi-Carrier Quadrature Amplitude Modulation*. New York: Wiley, 2000, p. 483.

[8] A. Bohdanowicz, G. J. M. Janssen, and S. Pietrzyk, "WideBand indoor and outdoor multipath channel measurements at 17 GHz," in *Proc. IEEE Vehicular Technology Conf.*, vol. 4, 1999, pp. 1998–2003.

[9] H. Hashemi, D. Tholl, and G. Morrison, "Statistical modeling of the indoor radio propagation channel—Part I," in *Proc. IEEE Vehicular Technology Conf.*, 1992, pp. 338–342.

[10] P. Nobles, D. Ashworth, and F. Halsall, "Indoor radiowave propagation measurements at frequencies up to 20 GHz," in *Proc. IEEE Vehicular Technology Conf.*, 1994, pp. 873–877.

[11] Th. S. Rappaport, *Wireless Communications*: Prentice Hall, 1996, p. 164.

[12] W. C. Y. Lee, *Mobile Cellular Telecommunications Systems*. New York: McGraw-Hill, 1989.

[13] K. Pahlavan and R. Ganesh, "Statistical characterization of a partitioned indoor radio channel," in *Proc. IEEE Int. Conf. Communication, ICC'92*, Chicago, IL, June 14–17, 1992, pp. 1252–1256.
[14] L. Talbi and G. Y. Delisle, "Experimental characterization of EHF multipath indoor radio channels," *IEEE J. Select. Areas Commun.*, vol. 14, pp. 431–439, Apr. 1996.
[15] T. S. Rappaport and C. D. McGillem, "UHF fading in factories," *IEEE J. Select. Areas Commun.*, vol. 7, pp. 40–48, Jan. 1989.
[16] T. S. Rappaport, "Indoor radio communications for factories of the future," *IEEE Commun. Mag.*, pp. 15–24, May 1989.
[17] A. F. Abou-Raddy and S. M. Elnoubi, "Propagation measurements and channel modeling for indoor mobile radio at 10 GHz," in *Proc. IEEE Vehicular Technology Conf.*, vol. 3, 1997, pp. 1395–1399.
[18] W. T. Webb, L. Hanzo, and R. Steele, "Bandwidth-efficient QAM schemes for Rayleigh fading channels," in *Proc. 5th Int. Conf. Radio Receivers and Associated Systems*, 1989, pp. 139–142.
[19] H. Hashemi, "The indoor radio propagation channel," *Proc. IEEE*, vol. 81, no. 7, pp. 943–968, July 1993.
[20] Th. S. Rappaport, *Wireless Communications*. Englewood Cliffs, NJ: Prentice-Hall, 1996, p. 166.
[21] S. Loredo, "Modelo de Canal Específico del Entorno para el Análisis y Simulación de Sistemas Vía Radio en Interiores," Ph.D. dissertation, Apr. 2, 2001.
[22] A. A. M. Saleh and R. A. Valenzuela, "A statistical model for indoor multipath propagation," *IEEE J. Select. Areas Commun.*, vol. SAC-5, Feb. 1987.
[23] K. Bury, *Statistical Distributions in Engineering*. Cambridge, U.K.: Cambridge Univ. Press, 1999.
[24] "AWACS Final Report," (ACTS program, AC228), AWACS/CIT/PM1/DS/P/015/b1, Sept. 1, 1998.

Manuel Lobeira Rubio was born in Santander, Spain, on July 17, 1977. He received the M.S degree in electrical engineering from the University of Cantabria, Spain, in 2000.

He is currently pursuing the Ph.D. degree in electrical engineering in the field of propagation for ultra wide-band communications from the same university, while working for ACORDE (Advanced Communications Research and Development), Santander, Spain. His main interests are in the indoor radio channel propagation study and its applications to the design of communication systems.

Ana García-Armada (M'95) was born in Santiago de Compostela, Spain, in 1970. She received the S.M. and Ph.D. degrees in electrical engineering, both from the Polytechnic University of Madrid, Spain, in 1994 and 1998, respectively.

She is currently with the Department of Signal Processing and Communications, University Carlos III of Madrid, Spain. Her main interests are in simulation of communication systems and multicarrier modulation techniques.

Rafael P. Torres (M'90) was born in Málaga, Spain, in 1961. He received his M.S. degree in physics from the University of Granada, Spain, in 1986 and the Ph.D. degree in telecommunications engineering from the Polytechnic University of Madrid (UPM), in 1990.

From 1986 to 1990, he was with the Radio Communication and Signal Processing Department of the UPM as a Research Assistant. During this time, he worked on numerical methods in electromagnetics, and its applications to design of passive microwave devices like radomes, circular polarizer, rotators, and planar lenses. He became an Associate Professor in the Department of Communication Engineering of the University of Cantabria, Spain, in 1990. Since then, he has participated in several projects about RCS computation, on board antennas analysis, electromagnetic compatibility, and radio-propagation. He is coauthor of a book about the CG-FFT method, author of several chapters in different books and papers, and about 60 conference contributions. His current research interests include numerical and high-frequency methods in electromagnetics applied to radio-propagation for wireless and mobile communications, as well as the simulation and design of new wireless communications systems.

José Luis García (M'74) was born in 1938. He received the M.Sc. degree from the University of Zaragoza, Spain, in 1964 and the Ph.D. degree from the University of Valladolid, in 1971, where he was Assistant Professor.

He joined the University of Cantabria, Spain, in 1973 first as professor and, some time later, as Full Professor. Subsequently, he became Head of the Department of Electronics and later of the Communication Engineering Department. Currently, he participates in projects of the third, fourth, and fifth Framework of the RTD Program of the European Union related to radiocommunication systems and projects for the European Space Agency. He has coordinated European projects within the HCM program and has been Technical Project Manager of other projects. He has collaborated with the European Commission in several projects. He has chaired projects such as ALFA projects coordinating European and Latin-American Universities. His current research area is wireless for indoor communications, WLAN and WPAN, including UWB devices and systems.

Dr. García has been a member of the Management and Steering Committees of several Conferences and Organizations.